Dynamic modeling of a jointed structure with two hinged-hinged slightly curved beams connected by elastic joints

Y.-J. Zhai [1,2], Z.-S. Ma [1,2], Q. Ding [1,2], X.-P. Wang [3]
[1] Tianjin University, School of Mechanical Engineering,
Tianjin 300350, China
e-mail: **zhisai.ma@tju.edu.cn**

[2] Tianjin Key Laboratory of Nonlinear Dynamics and Control,
Tianjin 300350, China

[3] China Academy of Launch Vehicle Technology,
Beijing 100076, China

Abstract
The investigations of jointed structures have attracted considerable attention, and current research mainly focuses on the dynamic characteristics of the straight-beam structures with joints, while sometimes the jointed structures are assembled by curved beams in engineering practice. Hence, this paper aims to propose a dynamic modeling method for a jointed structure with two hinged-hinged slightly curved beams (SCBs) connected by elastic joints. In this work a nonlinear dynamic model of a single SCB is first established, and then the global mode method is used to establish the nonlinear dynamic model of the jointed structure. Thereafter, the forced vibration responses of the jointed structure are calculated by successively using the Galerkin truncation method, harmonic balance method and pseudo arc-length method. Finally, case studies are carried out to validate the proposed modeling method and the results calculated by the proposed method are in good agreement with the results of finite element analysis, which demonstrates the accuracy of the proposed dynamic modeling method.

1 Introduction

The need for jointed structures is pervasive throughout the civil, manufacturing, and infrastructure engineering communities. The common jointed types involve bolted joints [1-12], welded joints [13-17] and pinned joints [18-22]. In recent years, there have been considerable investigations on the dynamic analysis of jointed structures to pursue more accurate modeling and meet the ever-increasing requirements of engineering structures.

As a kind of typical jointed structures, the multi-beam structures connected with joints have been gotten considerable attention. On the one hand, some investigations were conducted based on the finite element method. Song et al. [23] proposed an adjust Iwan beam element to represent the bolted joints and then the finite element model of the beam structures with bolted joints is established to obtain its nonlinear dynamic responses. Wang [10] proposed an improved nonlinear dynamic reduction method to investigate a bolted lap beam system and validated by comparing with the full order methods. Tan et al. [24] used the parametric finite element method to analyze the effects of external load and non-parallel bearing surface on a bolted lap beam and verified by static hysteresis test experiments. Wang et al. [25] developed a three-dimensional progressive damage model to investigate the failure mechanism of composite bolted joints subject to tensile loading by using the Abaqus software. Gan et al. [26] proposed a simplified joint-slippage model based on the component method to calculate the load-deformation relationship of bolted joints and then the model is verified by comparing with the results of finite element analysis and the results of corresponding

experiments. Zhan et al. [27] proposed a finite element modeling and updating method based on the strain frequency response function and its effectiveness was validated by a L-shaped jointed structure.

On the other hand, some investigations were conducted based on the approximate analytic solution or the semi-analytic solution. Ahmadian et al. [28] proposed a nonlinear analytical model for the joint interface parameter identification of a bolted lap beam with tip mass. This model was used to estimate the forced responses by adopting the multiple scale method and verified by corresponding experiments. Based on the Timoshenko beam theory, Adel et al. [29] proposed an analytical model for an assembled beam with nonlinear joints and investigated the effects of different parameters on the nonlinear responses of the assembled beam. Meisami et al. [30] proposed a novel analytical model for analyzing the nonlinear behaviors of a bolted flange joint and its accuracy was verified by the experimental and finite element results. In addition, Chen et al. [31] derived the nonlinear partial differential governing equations of a foldable multi-beam structure to investigate its saturation and jumping phenomena. Wei et al. [32] proposed a global mode method to establish the analytical model of multi-beam structures for obtaining the accurate global modes, and then a low-dimensional and high-accuracy model was derived by using the global modes. Thereafter, Wei et al. successfully applied the global mode method to the dynamic modeling and analysis of flexible structures connected with nonlinear joints [33], space manipulators [34], flexible spacecrafts [35], and a two-beam structure with nonlinear joints [36].

From the above, the existing investigations about multi-beam structures connected with joints mainly focus on the straight beams, while some multi-beam structures connected with joints may be curved in practice and the effects of the curvature are found to be significant and inevitable in the single curved beam structures. Lee et al. [37] investigated the anti-symmetric mode vibrations of a fixed-fixed curved beam subject to autoparameteric excitation. Thereafter, the nonlinear vibration behaviors of the single curved beam subject to base harmonic excitation were investigated in terms of sound radiation [38] and sound absorption [39]. Nayfeh et al. [40] proposed a modal hypothesis method to calculate the exact solution of the postbuckling beams with hinged-hinged, fixed-fixed, and fixed-hinged boundaries, respectively. Then, this method was applied to solve the nonlinear vibration isolation problem of a slightly curved beam (SCB) by Ding et al. [41]. Thereafter, Ye et al. [42] investigated the nonlinear behaviors of a SCB with nonlinear boundaries by using the harmonic balance method and the pseudo arc-length method. Based on the modal hypothesis method, Zhai et al. [43] proposed an analytical model of a SCB with hinged-hinged boundaries subject to axial loads, which focused on the effects of axial loads and initial configurations on the SCB and was verified by the corresponding finite element analysis.

In view of the significant effects of curvature on the SCB structure, this work aims to propose a novel modeling method for a jointed structure with two hinged-hinged SCBs connected by elastic joints based on the modelling method of the single SCB structures and the global mode method of the straight-beam jointed structures. The rest of this paper is organized as follows. The analytic models of a single SCB and a jointed structure with two hinged-hinged SCBs connected by elastic joints are respectively established and corresponding solving process of forced vibration responses are given in Section 2. Case studies are carried out to verify the proposed modeling method in Section 3. Concluding remarks are finally summarized in Section 4.

2 Dynamic modeling of a two-SCB structure connected with elastic joints

2.1 Dynamic equation of a single SCB

The schematic diagram of a hinged-hinged SCB is shown in Figure 1. The shape of the single SCB is sinusoidal, with L denoting the length, $w_0(x,t) = a\sin(\pi x/L)$ the initial configuration and a the initial curvature. The single SCB is excited by a transverse concentrated force $F(t) = F_0\cos(\omega_F t)$, with F_0 being the amplitude and ω_F the frequency. The transverse deformation of the single SCB is $w(x,t)$, where x and t denote the axial space coordinate and time coordinate, respectively.

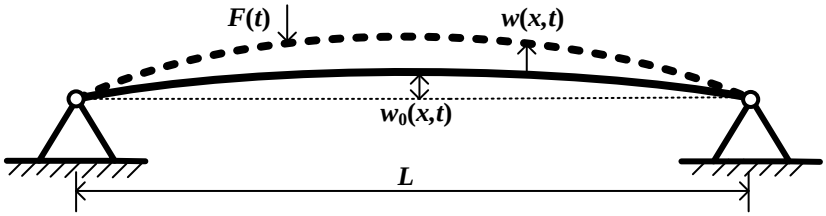

Figure 1: The schematic diagram of a hinged-hinged SCB

Based on the Euler-Bernoulli beam theory, the equation of motion of a single SCB is given as follows [40-43]

$$\rho A\ddot{w}+\eta\dot{w}+EIw''''+\xi I\dot{w}''''=\frac{EA}{2L}\left(w''+w_0''\right)\int_0^L\left(w'^2+2w'w_0'\right)dx+F_0\cos\left(\omega_F t\right) \tag{1}$$

The hinged-hinged boundary conditions can be described as

$$\begin{aligned} &w(0,t)=0, \qquad w(L,t)=0\\ &EIw''(0,t)=0, \quad EIw''(L,t)=0 \end{aligned} \tag{2}$$

The linear governing equation of the free vibration of the single SCB can be derived by dropping the damping terms, nonlinear terms and external excitation from (1), and shown as

$$\rho A\ddot{w}+EIw''''=\frac{EA}{2L}w_0''\int_0^L 2w'w_0'\,dx \tag{3}$$

The eigenvalue problem of equation (3) is first solved to obtain natural frequencies and mode shapes, which are needed for the subsequent discretization. Hence, assuming that the displacement of the single SCB is separable in space and time, the solution of equation (3) can be set as

$$w(x,t)=\varphi(x)e^{j\omega t} \tag{4}$$

with ω denoting the natural frequency and $\varphi(x)$ the mode function. Substituting the separable solutions (4) into (3) yields

$$-\omega^2\rho A\varphi(x)+EI\varphi''''(x)=\frac{EA}{2L}w_0''\int_0^L 2\varphi'(x)w_0'\,dx \tag{5}$$

Substituting the equation (4) into (2), the boundary conditions can be simplified as

$$\begin{aligned} &\varphi(0)=0, \qquad \varphi(L)=0\\ &EI\varphi''(0)=0, \quad EI\varphi''(L)=0 \end{aligned} \tag{6}$$

According to references [41-43], the general solution of non-homogeneous equation (5) can be rewritten as

$$\varphi(x)=A_1\cos(\beta x)+B_1\sin(\beta x)+C_1\cos h(\beta x)+D_1\sinh(\beta x)+E_1\sin\left(\frac{n\pi}{L}x\right) \tag{7}$$

Obviously, the general solution (7) is required to satisfy equation (5) and the boundary conditions given in equation (6). Hence, the equations can be written into matrix form as

$$\boldsymbol{H}(\omega)[A_1\ \ B_1\ \ C_1\ \ D_1\ \ E_1]^{\mathrm{T}}=0 \tag{8}$$

with $\boldsymbol{H}(\omega)$ denoting the matrix related to eigenvalues and $[A_1\ \ B_1\ \ C_1\ \ D_1\ \ E_1]^{\mathrm{T}}$ the coefficients to be solved. By solving equation $\det\left(\boldsymbol{H}(\omega)\right)=0$, the eigenvalues can be obtained and the coefficients are subsequently resolved.

The governing equation of the single SCB as given in equation (1) can be discretized into ordinary differential equations by using the Galerkin truncation method. The transverse displacements of the SCB can be written as

$$w(x,t)=\sum_{i=1}^{N}\varphi_i(x)\,q_i(t) \tag{9}$$

with N being the truncation order of the Galerkin truncation method, $\varphi_i(x)$ the trial functions and $q_i(t)$ the modal coordinates, respectively.

Substituting equation (9) into (1), multiplying the weight functions $\varphi_k(x)$, and integrating along the length of the SCB, the following equations can be derived according to the orthogonality of mode shapes

$$\begin{aligned}
&\rho A\int_0^L \varphi_k(x)\,\varphi_k(x)dx\,\ddot{q}_k(t)+EI\int_0^L \varphi_k(x)\,\varphi_k''''(x)dx\,q_k(t)\\
&+\eta\int_0^L \varphi_k(x)\,\varphi_k(x)dx\,\dot{q}_k(t)+\xi I\int_0^L \varphi_k(x)\,\varphi_k''''(x)dx\,\dot{q}_k(t)\\
&=\frac{EA}{2L}\int_0^L \varphi_k(x)\,\varphi_k''(x)dx\,q_k(t)\int_0^L\left(\left(\sum_{i=1}^{N}\varphi_i'(x)\,q_i(t)\right)^2+2\left(\sum_{i=1}^{N}\varphi_i'(x)\,q_i(t)\right)w_0'\right)dx\\
&+\frac{EA}{2L}\int_0^L \varphi_k(x)\,w_0''\,dx\int_0^L\left(\left(\sum_{i=1}^{N}\varphi_i'(x)\,q_i(t)\right)^2+2\left(\sum_{i=1}^{N}\varphi_i'(x)\,q_i(t)\right)w_0'\right)dx\\
&+F_0\cos(\omega_F t)\varphi_k(x-x_F)
\end{aligned} \tag{10}$$

where, $\varphi_k(x)$ takes the same form as $\varphi_i(x)$, with $k=1, 2, 3\ldots, N$. x_F represents the location of the transverse concentrated force. The forced vibration responses of equation (10) can be calculated by using the harmonic balance method and the pseudo arc-length method. It should be noticed that the response amplitude of the displacement takes the maximum value of the stable periodic solution of $w(x,t)$ in this work.

2.2 Dynamic equation of a two-SCB structure connected with elastic joints

The schematic diagram of a two-SCB structure connected with elastic joints is shown in Figure 2. Regarding the above jointed structure, the dynamic characteristics of the elastic joints are introduced into the global model of the jointed structure by applying the equilibrium conditions between the two SCBs and the joints, and the global mode method is subsequently used to obtain natural frequencies and mode shapes of the jointed structure.

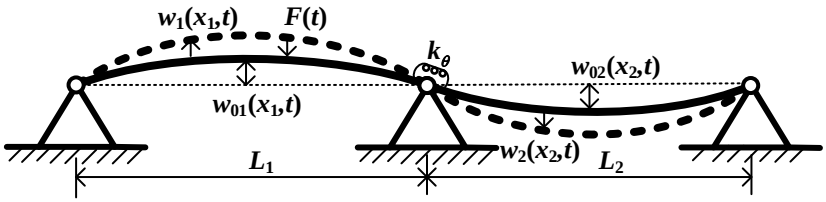

Figure 2: The schematic diagram of a two-SCB structure connected with elastic joints

Similar to equation (1), the equation of motion of the two SCBs are written as follows

$$\rho A\ddot{w}_i+\eta\dot{w}_i+EIw_i''''+\xi I\dot{w}_i''''=\frac{EA}{2L_i}\left(w_i''+w_{0i}''\right)\int_0^{L_i}\left(w_i'^{\,2}+2w_i'w_{0i}'\right)dx_i+F_0\cos(\omega_F t),\quad i=1,2 \tag{11}$$

The geometric, force and moment matching conditions at the location of the elastic joint are given as follows

$$\begin{aligned}
&w_1(L_1,t)=w_2(0,t)=0,\\
&EIw_1''(L_1,t)=EIw_2''(0,t)=k_\theta\left(w_2'(0,t)-w_1'(L_1,t)\right)
\end{aligned} \tag{12}$$

The corresponding boundary conditions are described as

$$\begin{aligned} &w_1(0,t)=0, \qquad w_2(L_2,t)=0 \\ &EIw_1''(0,t)=0, \;\; EIw_2''(L_2,t)=0 \end{aligned} \tag{13}$$

According to references [32-36], the global modes can be assumed as

$$w_i(x_i,t)=\varphi_i(x_i)e^{j\omega t}, \;\; i=1,2 \tag{14}$$

Substituting equation (14) into the free vibration equation of each SCB yields

$$-\omega^2\rho A\varphi_i(x_i)+EI\varphi_i''''(x_i)=\frac{EA}{2L_i}w_{0i}''\int_0^{L_i}2\varphi_i'(x_i)w_{0i}'\,dx_i, \;\; i=1,2 \tag{15}$$

Hence, the general solution of equation (15) can be solved as

$$\begin{aligned} \varphi_1(x_1)&=A_1\cos(\beta x_1)+B_1\sin(\beta x_1)+C_1\cos h(\beta x_1)+D_1\sinh(\beta x_1)+E_1\sin\left(\frac{n\pi}{L_1}x_1\right) \\ \varphi_2(x_2)&=A_2\cos(\beta x_2)+B_2\sin(\beta x_2)+C_2\cos h(\beta x_2)+D_2\sinh(\beta x_2)+E_2\sin\left(\frac{n\pi}{L_2}x_2\right) \end{aligned} \tag{16}$$

Substituting equation (16) into equations (12), (13) and (15), and writing the equations into matrix form yields

$$\tilde{\boldsymbol{H}}(\omega)_{10\times10}[\boldsymbol{\Psi}_1 \;\; \boldsymbol{\Psi}_2]^{\mathrm{T}}{}_{10\times1}=0 \tag{17}$$

where, $\boldsymbol{\Psi}_1=[A_1 \;\; B_1 \;\; C_1 \;\; D_1 \;\; E_1]^{\mathrm{T}}$ and $\boldsymbol{\Psi}_2=[A_2 \;\; B_2 \;\; C_2 \;\; D_2 \;\; E_2]^{\mathrm{T}}$. Then the global modes can be obtained by solving equation $\det\left(\tilde{\boldsymbol{H}}(\omega)_{10\times10}\right)=0$ and the coefficients are subsequently resolved.

By using the first N global mode shapes, the displacements of the jointed structure can be written as

$$w_i(x_i,t)=\sum_{j=1}^{N}\varphi_i^j(x_i)\,q_j(t) \;\; i=1,2 \tag{18}$$

Applying the Galerkin truncation method to equation (11), the low-dimensional nonlinear ordinary differential equations are obtained as follows

$$\begin{aligned} &\rho A\sum_{i=1}^{2}\int_0^{L_i}\left(\varphi_i^k(x_i)\varphi_i^k(x_i)dx_i\right)\ddot{q}_k(t)+EI\sum_{i=1}^{2}\int_0^{L_i}\left(\varphi_i^k(x_i)\varphi_i^{k''''}(x_i)dx_i\right)q_k(t) \\ &+\eta\sum_{i=1}^{2}\int_0^{L_i}\left(\varphi_i^k(x_i)\varphi_i^k(x_i)dx_i\right)\dot{q}_k(t)+\xi I\sum_{i=1}^{2}\int_0^{L_i}\left(\varphi_i^k(x_i)\varphi_i^{k''''}(x_i)dx_i\right)\dot{q}_k(t) \\ &=\sum_{i=1}^{2}\frac{EA}{2L_i}\int_0^{L_i}\varphi_i^k(x_i)\;\varphi_i^{k''}(x_i)dx_i\;q_k(t)\int_0^{L_i}\left(\left(\sum_{j=1}^{N}\varphi_i^{j'}(x_i)\,q_j(t)\right)^2+2\left(\sum_{j=1}^{N}\varphi_i^{j'}(x_i)\,q_j(t)\right)w_{0i}'\right)dx_i \\ &+\sum_{i=1}^{2}\frac{EA}{2L_i}\int_0^{L_i}\varphi_i^k(x_i)\;w_{0i}''\;dx_i\int_0^{L_i}\left(\left(\sum_{j=1}^{N}\varphi_i^{j'}(x_i)\,q_j(t)\right)^2+2\left(\sum_{j=1}^{N}\varphi_i^{j'}(x_i)\,q_j(t)\right)w_{0i}'\right)dx_i \\ &+F_0\cos(\omega_F t)\varphi_1^k(x_1-x_F) \end{aligned} \tag{19}$$

where, $\varphi_i^k(x_i)$ takes the same form as $\varphi_i^j(x_i)$ with $k=1, 2, 3\ldots, N$. x_F represents the location of the transverse concentrated force. The forced vibration responses of equation (19) can be calculated by using the harmonic balance method and the pseudo arc-length method.

3 Case studies and discussions

In this section, case studies are carried out to verify the proposed modeling method. According to reference [41-43], the partial differential equations can be discretized into ordinary differential equations by using the Galerkin truncation method with the truncation order being 4, and the forced vibration responses can be

calculated by applying the harmonic balance method with the harmonic order being 3. The material of the SCB is aluminum and corresponding physical parameter values are given in Table 1.

Table 1: Physical parameter values of an aluminum SCB

Item	Notation	Value
Length of a single SCB	$L = L_1 = L_2$	0.5 m
Height of the cross section	h	0.005 m
Width of the cross section	b	0.02 m
Young's modulus	E	68.9 GPa
Density	ρ	2800 kg/m^3
External damping coefficient	η	0 N s/m^2
Internal damping coefficient	ξ	2×10^7 N s/m^2

3.1 A single SCB with hinged-hinged boundaries

Firstly, a single SCB with hinged-hinged boundaries is analyzed and its schematic diagram has been presented in Figure 1. Figure 3(a) depicts the first four natural frequencies of the SCB affected by different initial curvature, which depicts that the first natural frequency of the SCB increases gradually with the increase of initial curvature and then exceeds the second natural frequency when the initial curvature exceeds around 0.008 m. Meanwhile, the initial curvature has little effects on the other three natural frequencies. Figure 3(b) depicts the first four mode shapes with the curvature being 0.003 m. In addition, the results of corresponding finite element analysis have been also depicted in Figure 3. It should be point out that the lines represent the results of the proposed method and the circles represent the results of corresponding finite element analysis. Evidently, the results calculated by the proposed method introduced in Section 2.1 are in good agreement with their counterparts by the finite element method, which verifies the accuracy of the modeling method for the single SCB with hinged-hinged boundaries.

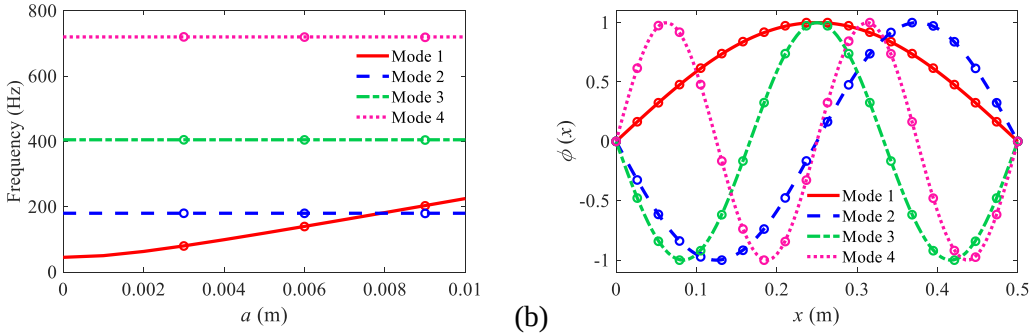

Figure 3: The first four natural frequencies and mode shapes of the single SCB

The forced vibration responses of the single SCB with hinged-hinged boundaries have been subsequently calculated and the corresponding analysis results have been depicted in the form of amplitude-frequency response curves in Figure 4. In Figure 4(a), the external excitation amplitude is constant with the value of 10 N, but the initial curvature respectively takes the value of 0.002, 0.003 and 0.004 m. The curves of Figure 4(a) illustrate that the hardening and softening nonlinear characteristics coexist, and the softening nonlinear characteristics become more dominant while the super-harmonic resonance is suppressed with the increase of the initial curvature. In Figure 4(b), the initial curvature is constant with the value of 0.003 m, but the external excitation amplitude respectively takes the value of 5, 10, 15 N. The curves of Figure 4(b) illustrate that the resonance intensity becomes larger and the nonlinear behaviors become more significant with the increase of the external excitation amplitude.

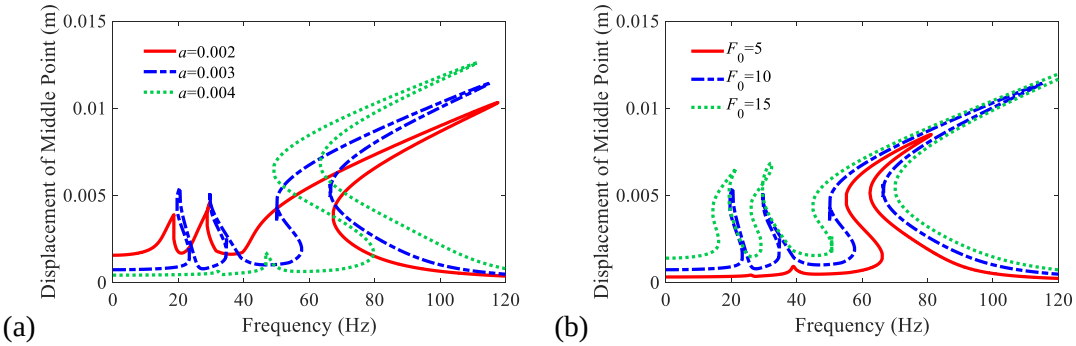

Figure 4: Amplitude-frequency curves of the single SCB affected by the initial curvature and external excitation amplitude

3.2 A jointed structure with two hinged-hinged SCBs connected by elastic joints

On the premise of ensuring the accurate modeling of the single SCB, a jointed structure with two hinged-hinged SCBs connected by elastic joints is analyzed and its schematic diagram has been presented in Figure 2. Regarding the jointed structure, natural frequencies and mode shapes of the jointed structure are first obtained, and Figure 5(a) depicts the first four natural frequencies of the jointed structure affected by different initial curvature. Figure 5(a) illustrates that the first two natural frequencies of the jointed structure increase gradually and even exceed the third and fourth natural frequencies with the increase of the initial curvature, while the initial curvature has little effects on the other two natural frequencies. Moreover, the first four mode shapes of the jointed structure with the initial curvature being 0.003 m are depicted in Figure 5(b). Thereafter, the results of corresponding finite element analysis are also depicted in Figure 5 and they are in good agreement with their counterparts by the proposed method introduced in Section 2.2, which further verifies the accuracy of the modeling method for the jointed structure with two hinged-hinged SCBs connected by elastic joints.

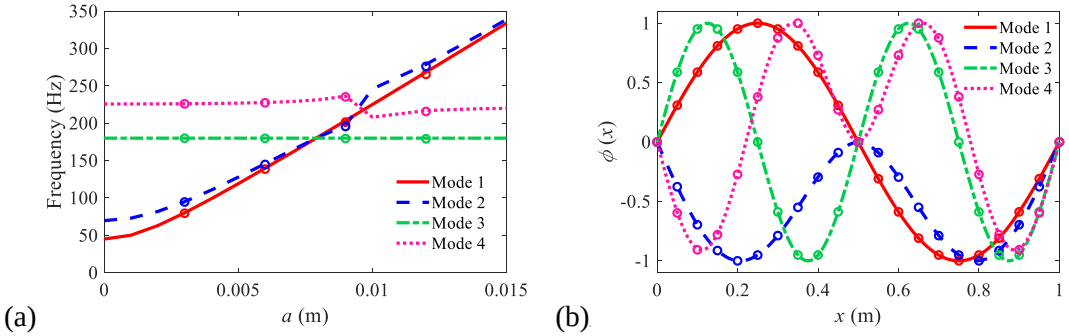

Figure 5: The first four natural frequencies and mode shapes of the jointed structure

Then, the forced vibration responses of the jointed structure with two hinged-hinged SCBs connected by elastic joints have been subsequently calculated and the corresponding analysis results have been depicted in the form of amplitude-frequency response curves in Figure 6. It should be point out that the results of the amplitude-frequency response curves in Figure 6 do not consider the coupling terms introduced by the nonlinear terms, that is, letting the superscript j be equal to the value of the superscript k in equation (19) . In Figure 6(a), the external excitation amplitude is constant with the value of 10 N, but the initial curvature respectively takes the value of 0.002, 0.003 and 0.004 m. The curves of Figure 6(a) illustrate that the hardening and softening nonlinear characteristics coexist at the first primary resonance, and the softening nonlinear characteristics become more dominant while the super-harmonic resonance is suppressed with the increase of the initial curvature. However, the nonlinear characteristics are not obvious at the second primary resonance. The second primary resonance peaks of the jointed structure shift to the right with the increase

of curvature, which is corresponding to the phenomena depicted in Figure 5(a). In Figure 6(b), the initial curvature is constant with the value of 0.003 m, but the external excitation amplitude respectively takes the value of 5, 10, 15 N. The curves of Figure 6(b) illustrate that the resonance intensity becomes larger and the nonlinear behaviors become more significant with the increase of the external excitation amplitude.

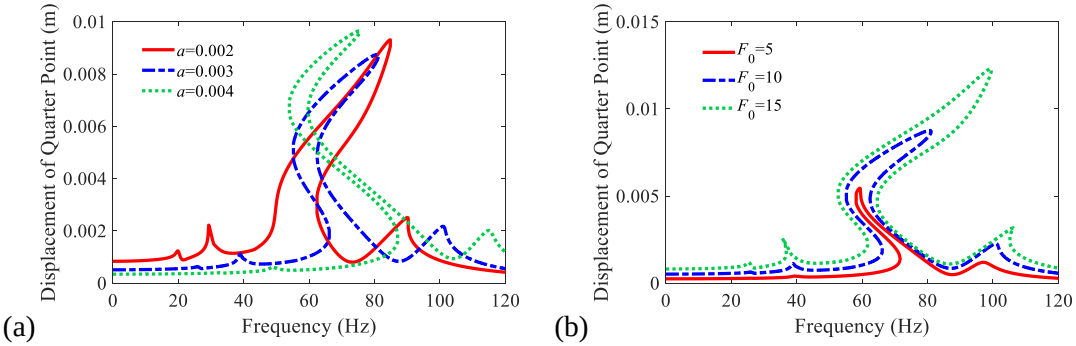

Figure 6: Amplitude-frequency curves of the jointed structure affected by the initial curvature and external excitation amplitude

4 Conclusions

This paper investigates the dynamic modeling method and nonlinear dynamic characteristic analysis of a jointed structure with two hinged-hinged SCBs connected by elastic joints. The analytic models of a single SCB and a jointed structure with two hinged-hinged SCBs connected by elastic joints are respectively established. The global mode method is successfully used to obtain natural frequencies and mode shapes of the above jointed structure, which was only applied to the modeling of straight-beam structures with joints in the existing research. Thereafter, corresponding forced vibration responses of the single SCB and the jointed structure are calculated by adopting the Galerkin truncation method, harmonic balance method and pseudo arc-length method. The effects of initial curvature and external excitation amplitude on the nonlinear dynamic characteristics of the single SCB and the jointed structure are analyzed by carrying out two case studies.

Some conclusions can be reached by analyzing the results of the case studies. Firstly, the increase of initial curvature has significant effects on one mode of the single SCB and two modes of the jointed structure but little effects on other modes. Secondly, the softening nonlinear characteristics become more dominant while the super-harmonic resonance is suppressed with the increase of the initial curvature. Thirdly, the resonance intensity becomes larger and the nonlinear behaviors become more significant with the increase of the external excitation amplitude.

Acknowledgements

This work was supported by the Natural Science Foundation of Tianjin City (Grant no. 21JCQNJC00360), the National Natural Science Foundation of China (Grant nos. 11802201, 11972245), the Aeronautical Science Foundation of China (Grant no. 2020Z009048001), and the Young Elite Scientists Sponsorship Program by Tianjin (Grant no. TJSQNTJ-2020-01).

References

[1] N. N. Balaji, T. Dreher, M. Krack, and M. R. W. Brake, “Reduced order modeling for the dynamics of jointed structures through hyper-reduced interface representation,” *Mechanical Systems and Signal Processing*, vol. 149, pp. 107249, 2021.

[2] W. Chen, D. Jana, A. Singh, M. Jin, M. Cenedese, G. Kosova, M. R. W. Brake, C. W. Schwingshackl, S. Nagarajaiah, K. J. Moore, and J.-P. Noël, "Measurement and identification of the nonlinear dynamics of a jointed structure using full-field data, Part I: Measurement of nonlinear dynamics," *Mechanical Systems and Signal Processing,* vol. 166, pp. 108401, 2022.

[3] R. de Oliveira Teloli, L. G. G. Villani, S. d. Silva, and M. D. Todd, "On the use of the GP-NARX model for predicting hysteresis effects of bolted joint structures," *Mechanical Systems and Signal Processing,* vol. 159, pp. 107751, 2021.

[4] N. Jamia, H. Jalali, J. Taghipour, M. I. Friswell, and H. Haddad Khodaparast, "An equivalent model of a nonlinear bolted flange joint," *Mechanical Systems and Signal Processing,* vol. 153, pp. 107507, 2021.

[5] M. Jin, G. Kosova, M. Cenedese, W. Chen, A. Singh, D. Jana, M. R. W. Brake, C. W. Schwingshackl, S. Nagarajaiah, K. J. Moore, and J.-P. Noël, "Measurement and identification of the nonlinear dynamics of a jointed structure using full-field data; Part II - Nonlinear system identification," *Mechanical Systems and Signal Processing,* vol. 166, pp. 108402, 2022.

[6] R. Lacayo, L. Pesaresi, J. Groß, D. Fochler, J. Armand, L. Salles, C. Schwingshackl, M. Allen, and M. Brake, "Nonlinear modeling of structures with bolted joints: A comparison of two approaches based on a time-domain and frequency-domain solver," *Mechanical Systems and Signal Processing,* vol. 114, pp. 413-438, 2019.

[7] R. M. Lacayo, and M. S. Allen, "Updating structural models containing nonlinear Iwan joints using quasi-static modal analysis," *Mechanical Systems and Signal Processing,* vol. 118, pp. 133-157, 2019.

[8] G. Li, Z. K. Nie, Y. Zeng, J. C. Pan, and Z. Q. Guan, "New Simplified Dynamic Modeling Method of Bolted Flange Joints of Launch Vehicle," *Journal of Vibration and Acoustics,* vol. 142, no. 2, pp. 1-13, 2020.

[9] R. d. O. Teloli, S. da Silva, T. G. Ritto, and G. Chevallier, "Bayesian model identification of higher-order frequency response functions for structures assembled by bolted joints," *Mechanical Systems and Signal Processing,* vol. 151, pp. 107333, 2021.

[10] D. Wang, "An improved nonlinear dynamic reduction method for complex jointed structures with local hysteresis model," *Mechanical Systems and Signal Processing,* vol. 149, pp. 107214, 2021.

[11] S. Wischmann, K. Seifert, J. Berroth, and G. Jacobs, "On the influence of surface sealant on the nonlinear dynamics of jointed structures," *Mechanical Systems and Signal Processing,* vol. 173, pp. 109061, 2022.

[12] P.-P. Yuan, W.-X. Ren, and J. Zhang, "Dynamic tests and model updating of nonlinear beam structures with bolted joints," *Mechanical Systems and Signal Processing,* vol. 126, pp. 193-210, 2019.

[13] S. Cai, Y. Zhang, J. Wu, and F. Wu, "A fuzzy finite element model based on the eigenstrain method to evaluate the welding distortion of T-joint fillet welded structures," *Journal of Manufacturing Processes,* vol. 77, pp. 451-462, 2022.

[14] P.-H. Liu, I. Y. Chen, X.-Q. Liu, C.-K. Su, C.-W. Hsu, D.-C. Dzeng, and Y.-C. Sung, "Stress influence matrix on hot spot stress analysis for welded tubular joint in offshore jacket structure," *Ocean Engineering,* vol. 251, pp. 111103, 2022.

[15] J. Xia, and H. Jin, "Analysis of residual stresses and variation mechanism in dissimilar girth welded joints between tubular structures and steel castings," *International Journal of Pressure Vessels and Piping,* vol. 165, pp. 104-113, 2018.

[16] V. Gupta, T. Lee, A. Vivek, K. S. Choi, Y. Mao, X. Sun, and G. Daehn, "A robust process-structure model for predicting the joint interface structure in impact welding," *Journal of Materials Processing Technology,* vol. 264, pp. 107-118, 2019.

[17] S. Chen, J. Liu, B. Chen, and X. Suo, "Universal fillet weld joint recognition and positioning for robot welding using structured light," *Robotics and Computer-Integrated Manufacturing,* vol. 74, pp. 102279, 2022.

[18] Y. Xue, Y. Wang, X. Xu, H.-P. Wan, Y. Luo, and Y. Shen, "Comparison of different sensitivity matrices relating element elongations to structural response of pin-jointed structures," *Mechanics Research Communications,* vol. 118, pp. 103789, 2021.

[19] X.-C. Wei, Y.-F. Liu, J.-S. Fan, X.-G. Liu, and S.-Y. Kong, "Safety assessment of existing pin-jointed grid structures with crooked members using static model updating," *Engineering Structures,* vol. 247, pp. 113107, 2021.

[20] Y.-Q. Xia, N. Xiao, H.-P. Chen, and X.-Q. Qian, "Determination of static and kinematic determinacy of pin-jointed assemblies using rigid-body displacements as primary unknown variables," *Engineering Structures,* vol. 181, pp. 643-652, 2019.

[21] F. Nouri, H. R. Valipour, and M. A. Bradford, "Finite element modelling of steel-timber composite beam-to-column joints with nominally pinned connections," *Engineering Structures,* vol. 201, pp. 109854, 2019.

[22] M. Mohammadi, and S. M. Motovali Emami, "Multi-bay and pinned connection steel infilled frames; an experimental and numerical study," *Engineering Structures,* vol. 188, pp. 43-59, 2019.

[23] Y. Song, C. J. Hartwigsen, D. M. McFarland, A. F. Vakakis, and L. A. Bergman, "Simulation of dynamics of beam structures with bolted joints using adjusted Iwan beam elements," *Journal of Sound and Vibration,* vol. 273, no. 1, pp. 249-276, 2004.

[24] L. Tan, C. Wang, Y. Liu, W. Sun, and W. Zhang, "Study on hysteresis and threaded fitting behavior of bolted joint with non-parallel bearing surface," *Mechanical Systems and Signal Processing,* vol. 168, pp. 108655, 2022.

[25] J. Wang, T. Qin, N. R. Mekala, Y. Li, M. Heidari-Rarani, and K.-U. Schröder, "Three-dimensional progressive damage and failure analysis of double-lap composite bolted joints under quasi-static tensile loading," *Composite Structures,* vol. 285, pp. 115227, 2022.

[26] Y.-d. Gan, H.-z. Deng, and C. Li, "Simplified joint-slippage model of bolted joint in lattice transmission tower," *Structures,* vol. 32, pp. 1192-1206, 2021.

[27] Z. Ming, G. Qintao, Y. Lin, and Z. Baoqiang, "Finite element model updating of jointed structure based on modal and strain frequency response function," *Journal of Mechanical Science and Technology,* vol. 33, no. 10, pp. 4583-4593, 2019.

[28] H. Ahmadian, and H. Jalali, "Identification of bolted lap joints parameters in assembled structures," *Mechanical Systems and Signal Processing,* vol. 21, no. 2, pp. 1041-1050, 2007.

[29] F. Adel, and M. Jamal-Omidi, "Vibration of nonlinear bolted lap-jointed beams using Timoshenko theory," *Archive of Applied Mechanics,* vol. 88, no. 6, pp. 981-997, 2018.

[30] F. Meisami, M. Moavenian, and A. Afsharfard, "Nonlinear behavior of single bolted flange joints: A novel analytical model," *Engineering Structures,* vol. 173, pp. 908-917, 2018.

[31] J. Chen, W.-H. Hu, and Q.-S. Li, "Nonlinear dynamics of a foldable multibeam structure with one to two internal resonances," *International Journal of Mechanical Sciences,* vol. 150, pp. 369-378, 2019.

[32] J. Wei, D. Cao, L. Wang, H. Huang, and W. Huang, "Dynamic modeling and simulation for flexible spacecraft with flexible jointed solar panels," *International Journal of Mechanical Sciences,* vol. 130, pp. 558-570, 2017.

[33] J. Wei, D. Cao, H. Huang, L. Wang, and W. Huang, "Dynamics of a multi-beam structure connected with nonlinear joints: modelling and simulation," *Archive of Applied Mechanics,* vol. 88, no. 7, pp. 1059-1074, 2018.

[34] J. Wei, D. Cao, L. Liu, and W. Huang, "Global mode method for dynamic modeling of a flexible-link flexible-joint manipulator with tip mass," *Applied Mathematical Modelling,* vol. 48, pp. 787-805, 2017.

[35] J. Wei, D. Cao, and H. Huang, "Nonlinear vibration phenomenon of maneuvering spacecraft with flexible jointed appendages," *Nonlinear Dynamics,* vol. 94, no. 4, pp. 2863-2877, 2018.

[36] J. Wei, T. Yu, D. Jin, M. Liu, Y. Tian, and D. Cao, "Three-to-one internal resonance in a two-beam structure connected with nonlinear joints," *Archive of Applied Mechanics,* vol. 91, no. 9, pp. 3835-3850, 2021.

[37] Y. Y. Lee, W. Y. Poon, and C. F. Ng, "Anti-symmetric mode vibration of a curved beam subject to autoparametric excitation," *Journal of Sound and Vibration,* vol. 290, no. 1, pp. 48-64, 2006.

[38] Y. Y. Lee, R. K. L. Su, C. F. Ng, and C. K. Hui, "The effect of modal energy transfer on the sound radiation and vibration of a curved panel: Theory and experiment," *Journal of Sound and Vibration,* vol. 324, no. 3, pp. 1003-1015, 2009.

[39] Y. Y. Lee, J. L. Huang, C. K. Hui, and C. F. Ng, "Sound absorption of a quadratic and cubic nonlinearly vibrating curved panel absorber," *Applied Mathematical Modelling,* vol. 36, no. 11, pp. 5574-5588, 2012.

[40] A. H. Nayfeh, and S. A. Emam, "Exact solution and stability of postbuckling configurations of beams," *Nonlinear Dynamics,* vol. 54, no. 4, pp. 395-408, 2008.

[41] H. Ding, and L.-Q. Chen, "Nonlinear vibration of a slightly curved beam with quasi-zero-stiffness isolators," *Nonlinear Dynamics,* vol. 95, no. 3, pp. 2367-2382, 2019.

[42] S. Q. Ye, X. Y. Mao, H. Ding, J. C. Ji, and L. Q. Chen, "Nonlinear vibrations of a slightly curved beam with nonlinear boundary conditions," *International Journal of Mechanical Sciences,* vol. 168, pp. 105294, 2020.

[43] Y. J. Zhai, Z. S. Ma, Q. Ding, X. P. Wang, and T. Wang, "Nonlinear transverse vibrations of a slightly curved beam with hinged-hinged boundaries subject to axial loads," *Archive of Applied Mechanics,* vol. 92, no. 7, pp. 2081-2094, 2022.